CERN-TH.5536/89

FORWARD-BACKWARD ASYMMETRIES

Convenors: M. Böhm[3], W. Hollik[7]

Participants: D. Bardin[1], W. Beenakker[2], F.A. Berends[2], M. Bilenky[1], G. Burgers[4], J.E. Campagne[5], A. Djouadi[6], O. Fedorenko[1], S. Jadach[8], G. Montagna[9], O. Nicrosini[9], T. Riemann[10], M. Sachwitz[10], L. Trentadue[11], W.L. van Neerven[2], Z. Was[12], R. Zitoun[5]

ABSTRACT

An overview is given of the evaluation of the forward-backward asymmetry A_{FB} in $e^+e^- \to f\bar{f}$ around the Z peak. Numerical results for A_{FB} are presented with one-loop electroweak corrections and QED corrections with the $O(\alpha^2)$ leading contributions and soft photons resummed to all orders. The results of independent calculations agree better than $\Delta A_{FB} = 0.001$.

To appear in the Proceedings of the Workshop on Z Physics at LEP, edited by G. Altarelli, R. Kleiss and C. Verzegnassi

---

[1] J.I.N.R., Dubna, U.S.S.R.
[2] Instituut Lorentz, University of Leiden, Leiden, The Netherlands.
[3] Physikalisches Institut, Universität Würzburg, Würzburg, FRG.
[4] NIKHEF-H, Amsterdam, The Netherlands.
[5] LPNHE, Universités Pierre et Marie Curie et Paris VIII, Paris France.
[6] Inst. für Theoretische Physik RWTH Aachen, Aachen, FRG.
[7] CERN, Geneva, Switzerland.
[8] Institute of Physics, Jagellonian University, Krakow, Poland.
[9] INFN, Sezione di Pavia and Dipartimento di Fisica Nuclear et Teorica dell'Università, Pavia, Italy.
[10] Institut für Hochenergiephysik, Berlin-Zeuthen, GDR.
[11] Dipartimento di Fisica dell'Università, Parma, INFN, Gruppo Collegato di Parma, Sezione di Milano, Italy.
[12] Max-Planck-Institut für Physik und Astrophysik, München, FRG.

CERN-TH.5536/89
September 1989

Contents

1 Introduction

The measurement of the Z line shape will provide accurate values for the mass M_Z and width Γ_Z of the Z boson. When M_Z will be used as an input parameter the total and partial decay widths are predicted by the minimal model, therefore allowing tests of the underlying theory. Besides the Z line shape, the forward-backward asymmetry A_{FB} in $e^+e^- \to f\bar{f}$ (where $f = \mu, \tau, q$) is one of the most important quantities since it is sensitive to the weak mixing angle which is also a prediction of the minimal model after M_Z is known.

The main interest so far has been concentrated on A_{FB} for muon pair production with a long list of contributions by various authors [1-15]. If lepton universality holds the theoretical situation is the same as for τ pair production. But also asymmetries for quark pairs in the final state have become of experimental interest for LEP [16]. The formal theoretical treatment is quite similar to the lepton case and will be included here.

It is the purpose of this presentation to give an overview of the evaluation of A_{FB} with the aim of obtaining a theoretical accuracy of about 0.001. Our presentation is organized as follows: first we give definitions and the results in lowest order. This is followed by a classification and organization of the radiative corrections and their specific problems. Then the weak radiative corrections which are not of the bremsstrahlung type are discussed, afterwards the $O(\alpha)$ QED (photonic) corrections, and finally the higher order QED corrections. Comparisons between the results of independent calculations will also be performed checking the reliability of the present status.

2 Definitions, lowest order results

In order to define the notation we start with the well-known lowest order results for the differential cross section for the reaction $e^+e^- \to f\bar{f}$ ($f \neq e$). Figure 1 shows the kinematics and the diagrams which contribute in lowest order (Higgs exchange is negligible for the known fermions).

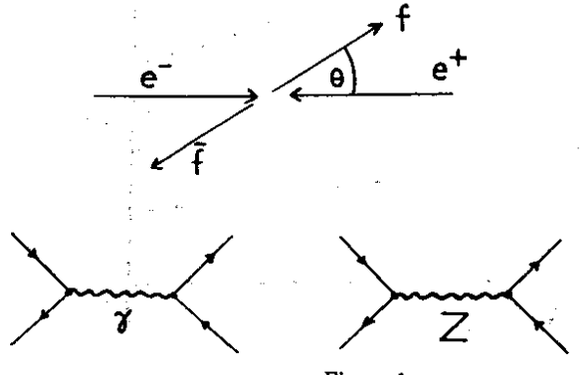

Figure 1:
Kinematics and lowest order diagrams in $e^+e^- \to f\bar{f}$

The forward-backward asymmetry is defined by

$$A_{FB} = \frac{\sigma_F - \sigma_B}{\sigma_F + \sigma_B} \tag{1}$$

with

$$\sigma_F = 2\pi \int_0^1 d(\cos\theta)\,\frac{d\sigma}{d\Omega}\,, \quad \sigma_B = 2\pi \int_{-1}^0 d(\cos\theta)\,\frac{d\sigma}{d\Omega}\,. \tag{2}$$

The lowest order expression for the differential cross section contains the Z propagator (normalized to the photon propagator)

$$\chi_0(s) = \frac{s}{s - M_Z^2 + iM_Z\Gamma_Z^0}\,, \tag{3}$$

and the Z-fermion vector and axial vector couplings (Q_f and I_3^f denote charge and weak isospin of the fermion f)

$$v_f = \frac{I_3^f - 2s_W^2\,Q_f}{2s_W c_W}\,, \quad a_f = \frac{I_3^f}{2s_W c_W}\,, \tag{4}$$

$$s_W \equiv \sin\theta_W\,, \quad c_W \equiv \cos\theta_W = M_W/M_Z\,, \tag{5}$$

and can be written in the following way ($N_C^f = 1, 3$ for f =lepton, quark; $\mu_f = m_f^2/s$):

$$\frac{d\sigma}{d\Omega} = \frac{\alpha^2}{4s}\,N_C^f\,\sqrt{1-4\mu_f}\quad \Big[G_1(s)\cdot(1+\cos^2\theta) + G_3(s)\cdot 2\cos\theta\cdot\sqrt{1-4\mu_f} \quad (6)$$
$$+G_2(s)\cdot\sin^2\theta\cdot 4\mu_f\Big]$$

where

$$\begin{aligned} G_1(s) &= Q_e^2Q_f^2 + 2Q_eQ_fv_ev_f\mathrm{Re}\,\chi_0(s) + (v_e^2+a_e^2)(v_f^2+a_f^2-4\mu_f a_f^2)\mid\chi_0(s)\mid^2 \quad (7)\\ G_2(s) &= Q_e^2Q_f^2 + 2Q_eQ_fv_ev_f\mathrm{Re}\,\chi_0(s) + (v_e^2+a_e^2)v_f^2\mid\chi_0(s)\mid^2\\ G_3(s) &= 2Q_eQ_fa_ea_f\mathrm{Re}\,\chi_0(s) + 4v_ea_ev_fa_f\mid\chi_0(s)\mid^2\,. \end{aligned}$$

This gives for the asymmetry in lowest order:

$$A_{FB}^0 = \frac{3}{4}\,\frac{G_3(s)}{G_1(s)+2\mu_fG_2(s)}\,\sqrt{1-4\mu_f}\,. \tag{8}$$

For the on-resonance asymmetry ($s = M_Z^2$) :

$$A_{FB}^0(M_Z^2) = \frac{3}{4}\,\frac{2v_ea_e\cdot 2v_fa_f\cdot\sqrt{1-4\mu_f}}{(v_e^2+a_e^2)(v_f^2+a_f^2)+\mu_f(v_e^2+a_e^2)(2v_f^2-4a_f^2)+\left(\frac{\Gamma_Z}{M_Z}\right)^2Q_f^2(1+2\mu_f)}\,. \tag{9}$$

For light fermions ($m_f/M_Z \ll 1$), and neglecting the $(\Gamma_Z/M_Z)^2$ terms from the γ exchange this simplifies to

$$A_{FB}^0(M_Z^2) = \frac{3}{4}\,A_e\,A_f \tag{10}$$

with

$$A_f = \frac{2v_fa_f}{v_f^2+a_f^2} = \frac{2(1-4\mid Q_f\mid s_W^2)}{1+(1-4\mid Q_f\mid s_W^2)^2}\,. \tag{11}$$

The combination (11) of coupling constants is displayed in figure 2 for the various fermion species.

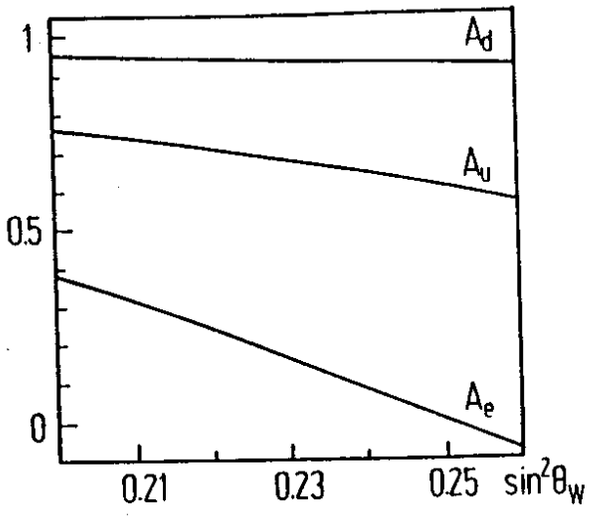

Figure 2:
The quantity A_f for quarks and leptons

Experimental errors [16]: The expected experimental accuracy for A_{FB} on resonance in the various fermion channels is listed in table 1, together with the error following for a measurement of the weak mixing angle.

	μ	b	c	s	u
ΔA_{FB}	0.0035	0.0055	0.007	0.007	0.014
$\Delta\sin^2\theta_W$	0.0017	0.0010	0.0015	0.0012	0.003

Table 1:
Error of A_{FB} and precision in $\sin^2\theta_W$ for various fermions

In view of these experimental errors, the finite mass effects are negligible even for b quarks where they reduce the value for A_{FB} by not more than 0.0005 compared to the

$m_b = 0$ approximation. Also the γ exchange contribution is only of marginal importance on top of the resonance. This means that in lowest order the on-resonance asymmetry is determined exclusively by the value of $\sin^2\theta_W$.

3 The structure of radiative corrections

The dependence of A_{FB} on only a single parameter is changed after including higher order contributions:

$$A_{FB} = A^0_{FB} + \Delta A^{RC}_{FB}. \tag{12}$$

The radiative correction term ΔA^{RC}_{FB} is generated by the loop diagrams contributing to the elastic cross section and the real photon bremsstrahlung emission as an inclusive inelastic process. ΔA^{RC}_{FB} depends on all parameters of the model. Since the physical input

$$\alpha,\ M_Z,\ M_W,\ M_H,\ m_f$$

is most clear in the on-shell scheme [see also the contribution on 'Electroweak Radiative corrections' to this report] we will utilize this scheme as a basis for the following discussion. Remember that the mixing angle is always to be understood as

$$\sin^2\theta_W = s^2_W = 1 - M^2_W/M^2_Z\,.$$

For the process $e^+e^- \to f\bar{f}$ the electroweak radiative corrections can be divided quite naturally into the following subclasses:

1. "QED corrections" (bremsstrahlung corrections) with an additional photon line in each Born diagram, either virtual or real (figure 3).
2. "Weak corrections", which collect all the other electroweak diagrams (schematically in figures 4-5).

Each class has its own characteristic features:

QED corrections:

- are dependent on the details of the experiment,
- are independent of the detailed structure of the underlying non-electromagnetic part of the theory,
- are gauge invariant and UV finite by themselves after QED renormalization,
- their coupling strength is determined by the low energy α,
- they need (together with the external fermion masses) only the global parameters M_Z, Γ_Z, v_f, a_f as input, without restriction to the Standard Model,
- they are large around the Z and consequently require a careful treatment including the leading higher order corrections.

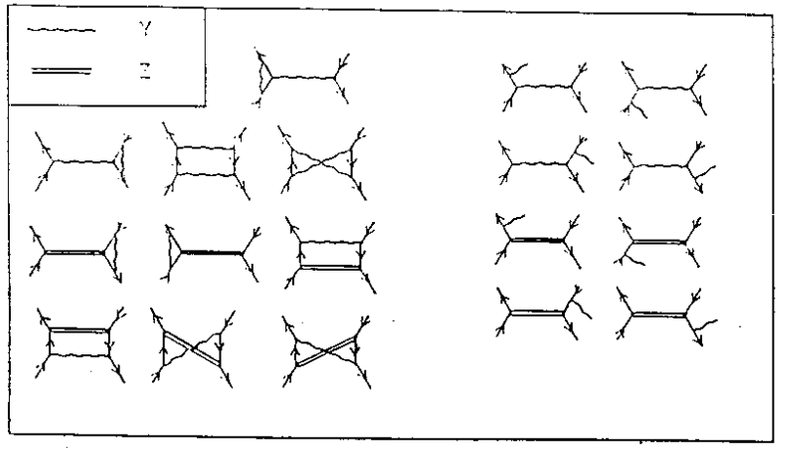

Figure 3: QED corrections to $e^+e^- \to \mu^+\mu^-$

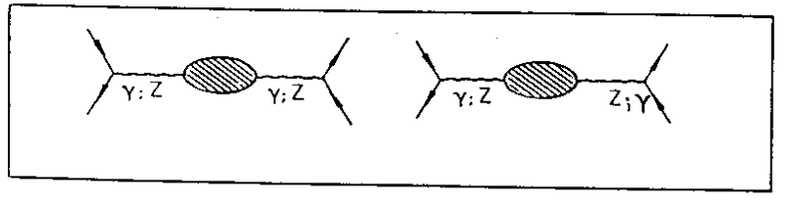

Figure 4: Propagator corrections to $e^+e^- \to \mu^+\mu^-$

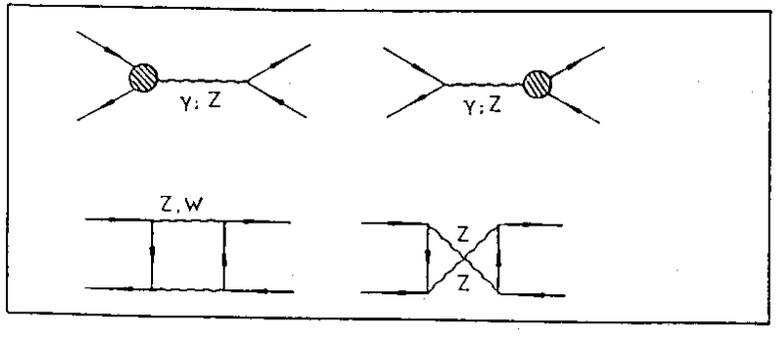

Figure 5: Vertex corrections and box contributions to $e^+e^- \to \mu^+\mu^-$

Weak corrections:

- are independent of the experimental set-up,
- are dependent on the detailed internal structure of the theory, in the Standard Model also on the non-Abelian structure and the Higgs sector; in particular they depend on the unknown parameters M_H, m_t. All building blocks necessary to guarantee the renormalizability of the Standard Model show up here; consequently,
- they have a complex structure and their treatment requires a good organization.

The numerically most important part of the weak corrections are the self-energy insertions in the gauge boson propagators (see the contribution on "Electroweak Radiative Corrections"). We will describe the detailed effects of the various subclasses on the asymmetry in the next section.

Muon decay:

A third class of important radiative corrections has not directly to do with $e^+e^- \to f\bar{f}$ processes: the corrections to the muon lifetime which are needed when the precisely known muon decay constant G_μ is used as an input data point. They enter the relation between G_μ, M_W, M_Z in terms of the quantity Δr [17] as follows (see also contribution "Δr", this report):

$$M_W^2\left(1-\frac{M_W^2}{M_Z^2}\right) = \frac{\pi\alpha}{\sqrt{2}G_\mu}\cdot\frac{1}{1-\Delta r}. \tag{13}$$

Via the loop diagrams to the W propagator all masses of the Standard Model are present in Δr. Any elimination of M_W resp. s_W^2 in favour of the precisely known G_μ will therefore depend on specific assumptions on the top mass and the Higgs mass. Note, however, that $\sin^2\theta_W$, as derived from (13) for given M_Z, M_H, m_t, is not the effective mixing angle which determines the asymmetries at the Z peak. The coupling constants and thus the asymmetries get additional contributions by the $\gamma - Z$ mixing and the vertex corrections.

According to our strategy for the discussion of the radiative corrections to the asymmetry A_{FB} the first important step is to establish the non-QED part. Afterwards, the QED contributions to $O(\alpha)$ have also to be settled before the higher order QED terms will be incorporated. A step-by-step comparison between the results of different groups will show that a sastisfactory consensus on the numbers has been obtained.

In addition to the electroweak corrections, the quark final states get **QCD corrections**, which are formally similar to the final state QED corrections. Hence they will be discussed together with these QED terms in section 5.3.

4 Weak corrections to A_{FB}

After this qualitative description we briefly put together the main features of the non-QED corrections followed by numerical results. A discussion of the ingredients at full length is given in the "Electroweak Radiative Corrections"contribution.

4.1 Propagator corrections

For processes with light external fermions ($f \neq t$) we need only the corrections to the γ and Z propagators. They are contained in the renormalized one-loop self energies $\hat{\Sigma}_{\gamma\gamma}$, $\hat{\Sigma}_{ZZ}$, $\hat{\Sigma}_{\gamma Z}$ and allow us to formulate the matrix element in a simple and transparent way by replacing the free propagators of the lowest order calculation by dressed ones:

- photon exchange amplitude:

$$\frac{e^2}{s} \to \frac{e^2}{s+\hat{\Sigma}_{\gamma\gamma}(s)} = \frac{1}{s}\cdot\frac{e^2}{1+\Pi_{\gamma\gamma}(s)} \tag{14}$$

- Z exchange amplitude including the Z self-energy with the 2-loop contribution to the imaginary part (i.e. corrections to the Z width):

$$\begin{aligned}\frac{e^2}{4s_W^2c_W^2}\cdot\frac{1}{s-M_Z^2+iM_Z\Gamma_Z^0} &\to \frac{e^2}{4s_W^2c_W^2}\cdot\frac{1}{s-M_Z^2+\Sigma_Z(s)} \\ &= \frac{e^2}{4s_W^2c_W^2}\cdot\frac{1}{1+\Pi_Z(s)}\cdot\frac{1}{s-M_Z^2+i\frac{s}{M_Z^2}M_Z\Gamma_Z}\end{aligned} \tag{15}$$

with

$$\Pi_Z(s) = \frac{\mathrm{Re}\Sigma_Z(s)}{s-M_Z^2} \tag{16}$$

and

$$M_Z\Gamma_Z = \frac{\mathrm{Im}\,\Sigma_Z(M_Z^2)+M_Z\Delta\Gamma_Z}{1+\Pi_Z(M_Z^2)}. \tag{17}$$

Γ_Z is now the physical width of the Z (containing electroweak corrections, QED corrections, and 3-particle decays). For the various quantities in the formulae above see "Electroweak Radiative Corrections".
These diagonal propagator corrections affect only the internal boson lines in a matrix element, independent of the quantum numbers of the external fermions.

- photon - Z mixing:
The insertion of the $\gamma - Z$ mixing propagator is associated with the electric charge of the external fermions, but in such a way that it can be absorbed by a redefinition of the mixing angle (if the imaginary part is dropped):

$$\bar{s}_W^2 = s_W^2 - s_W c_W \mathrm{Re}\frac{\Pi_{\gamma Z}(s)}{1+\Pi_{\gamma\gamma}(s)}. \tag{18}$$

This modifies the weak neutral vector current according to

$$J_\mu^{(f)} - \bar{J}_\mu^{(f)} = \gamma_\mu(I_3^f - 2\bar{s}_W^2Q_f). \tag{19}$$

Interpreted in this way, the $\gamma - Z$ mixing is also a universal contribution.

Many details of the Z propagator concerning normalization and width which are important for the line shape nearly cancel in the on-resonance asymmetry as a ratio of cross sections; they enter A_{FB} only together with the photon exchange and photon-Z interference, and hence are suppressed typically of the order $O(\frac{\Gamma}{M} \cdot \frac{\alpha}{\pi})$.

The structure of the amplitudes in (14) and (15) leads to the following pattern of running couplings absorbing the real parts of the self energies

$$\begin{aligned} e^2(s) &= \frac{e^2}{1 + \mathrm{Re}\Pi_{\gamma\gamma}(s)} \\ \left(\frac{e^2}{4s_W^2 c_W^2}\right)(s) &= \frac{e^2}{4s_W^2 c_W^2} \cdot \frac{1}{1 + \Pi_Z(s)} = \sqrt{2} G_\mu M_Z^2 \frac{1 - \Delta r}{1 + \Pi_Z(s)}, \end{aligned}$$

and the imaginary parts have to be inserted separately. The light fermions enter $\Pi_Z(s)$ in the same way as the photon vacuum polarization at the Z scale (see "Electroweak Radiative Corrections")

$$\Pi_Z(s) = \mathrm{Re}\,\Pi_{\gamma\gamma}(M_Z^2) + (\text{non-leading terms}).$$

This demonstrates that e in the NC coupling has to be evaluated at the Z mass scale. Equivalent: by using G_μ the large contribution from the vacuum polarization drops out.

By using effective coupling constants one should not forget that the propagator corrections are complex and also the imaginary parts give non-negligible effects: for example, in case of muons the contributions is (at $M_Z = 91$ GeV)

$$\Delta A_{FB}^{imag} \simeq +0.002.$$

4.2 Weak vertex corrections and box diagrams

The residual set of the 1-loop corrections consists of the vertex corrections to the electromagnetic and weak NC vertex (excluding virtual photons) and box diagrams with two Z and W bosons. For the known fermions the vertex corrections can be represented in terms of s dependent vector and axial vector form factors. The boxes allow a similar decomposition but with form factors depending on both s and t. In contrast to the class 4.1 these form factors are not universal but depend explicitly on the quantum numbers of the external fermions. For an explicit discussion see the "Electroweak Radiative Corrections"contribution.

On the other hand, for the light fermions $f \neq b, t$ they are exclusively determined by M_Z and M_W (neglecting Yukawa couplings) and are free of uncertainties coming from the presently unkown parameters of the standard model.

For $e^+e^- \to b\bar{b}$ the top quark appears also in the vertex and box diagrams [18], whereas the physical Higgs contribution is still suppressed by the smallness of the Yukawa couplings. Only for external fermions with masses comparable to those of the gauge bosons do these Higgs contributions become of importance.

Summarizing sections 4.1 and 4.2, the on-resonance asymmetry including weak corrections retains a simple structure, similar to the lowest order:

$$A_{FB} = \frac{3}{4} \bar{A}_e \bar{A}_f + \Delta A_{FB}^{imag} + \Delta A_{FB}^{vertex,box} \qquad (20)$$

where

$$\bar{A}_f = \frac{2(1 - 4 \mid Q_f \mid \bar{s}_W^2)}{1 + (1 - 4 \mid Q_f \mid \bar{s}_W^2)^2} \qquad (21)$$

and ΔA_{FB}^{imag} is the contribution from the imaginary parts in the propagator corrections. The non-universal contribution $\Delta A_{FB}^{vertex,box}$ and its dependence on s_W^2, the only one at $s = M_Z^2$, is presented in table 2. Table 3 contains the vertex contributions after determining the mixing angle from G_μ and Δr, eq. (13), which makes the vertex corrections also for the light fermions slightly top mass dependent. Note that the compensation between ΔA_{FB}^{imag} and $\Delta A_{FB}^{vertex,box}$ in (20) is accidental for muons and does not apply to the quark asymmetries.

s_W^2	$\mu^+\mu^-$	$u\bar{u}$	$d\bar{d}$
0.21	- 0.0028	- 0.0035	- 0.0039
0.22	- 0.0023	- 0.0034	- 0.0040
0.23	- 0.0017	- 0.0033	- 0.0041
0.24	- 0.0011	- 0.0031	- 0.0041
0.25	- 0.0004	- 0.0028	- 0.0042

Table 2:
$\Delta A_{FB}^{vertex,box}$ on resonance, dependence on s_W^2

m_t (GeV)	$\mu^+\mu^-$	$u\bar{u}$	$d\bar{d}$	$b\bar{b}$
50	- 0.0013	- 0.0028	- 0.0041	- 0.0041
100	- 0.0015	- 0.0033	- 0.0043	- 0.0043
150	- 0.0018	- 0.0035	- 0.0044	- 0.0047
200	- 0.0022	- 0.0038	- 0.0045	- 0.0055
230	- 0.0025	- 0.0040	- 0.0047	- 0.0063

Table 3:
$\Delta A_{FB}^{vertex,box}$ on resonance, dependence on m_t. $M_Z = 91$ GeV, $M_H = 100$ GeV.

4.3 Numerical results

Fixing M_W in terms of G_μ, α, M_Z, M_H, m_t by means of (13) leads directly to a prediction for A_{FB} which depends, after M_Z has been measured, on M_H and m_t. The corresponding results are displayed in figures 6,7 for the muon and b-quark asymmetries.

In an intermediate step, the effective mixing angle $\bar{s}^2_W$ is also a prediction which collects the unknown parameters and determines A_{FB} in terms of (20) and (21). The rest of the corrections, contained in $\Delta A_{FB}^{vertex,box}$, is (practically) free of M_H and m_t. This is also true for the exceptional case of $b\bar{b}$ final states since the additional top contribution in the vertex is below the experimental sensitivity (see table 3).

This has an important consequence. One and the same value of $\bar{s}^2_W$ determines A_{FB} for all kinds of fermions in the final state according to (20) and (21); moreover, it determines also the τ polarization asymmetry

$$A^\tau_{pol} = \bar{A}_e + \Delta A^{imag}_{pol} + \Delta A^{vertex,box}_{pol} .$$

This means that there is a relation between the various asymmetries which is independent of the Higgs and the top mass within the experimental errors. This relation is shown in figure 8. It is a rather general feature following from the gauge group SU(2)×U(1) and the usual fermion classification in the minimum representation and is not restricted to the minimal model. An experimentally observed violation of this relation would be a strong indication for new structures of the type SU(2)×U(1)×G which allow, for example, an admixture of a second Z boson in the on-resonance neutral current.

On the other hand, an experimental verification does not yet answer the question whether the minimal model is realized. For this second step the absolute predictions for the asymmetries are required as well as their relation to the measured W mass. These absolute predictions, however, do depend on our assumptions on M_H and m_t and hence are not unique as yet.

Now we want to compare the results obtained by different authors. The method of calculating the muon forward-backward asymmetry parametrized in terms of M_H and m_t has been applied by Lynn and Stuart [8], Hollik [19], and the Dubna-Zeuthen group, Bardin et al. [12,20]. The tables in [8] contain the integrated asymmetry for μ pair production for various top and Higgs masses. But compared to the more actual version by Kennedy et al. [14] they differ slightly due to a smaller hadronic vacuum polarization part (given as -0.0274 instead of -0.0288) and the incorporation of only the diagonal self-energy terms in the Z propagator. These higher order terms, which become of some significance for large top masses, are incorporated in the results of [14] and [19] (see also the discussion in "Electroweak Radiative Corrections"). They give rise to differences in the asymmetry for $e^+e^- \to \mu^+\mu^-$ if the top is heavy: 0.0005 for $m_t = 200$ GeV and 0.0015 for $m_t = 230$ GeV. Otherwise, the agreement is within 0.003 (after adapting the vacuum polarization part).

The calculation by Bardin et al. [12,20] was performed in the unitary gauge. As shown for the angular distributions in table 4 for the muon case, there is very good agreement between the results of [19] and [12,20]. For reasons of comparison the $O(\alpha^2)$

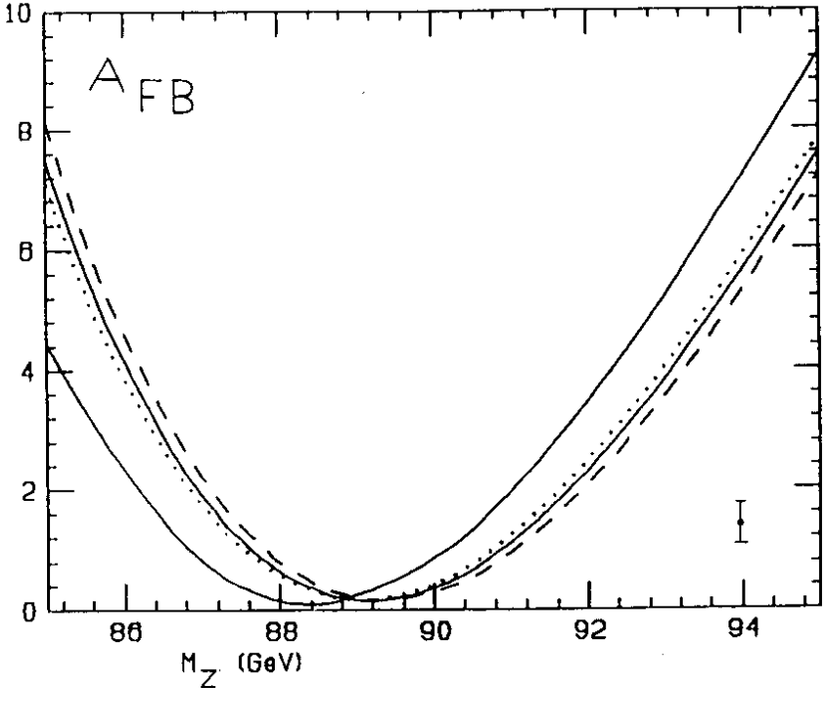

Figure 6:
A_{FB} for $e^+e^- \to \mu^+\mu^-$ in %, $s = M_Z^2$. No QED corrections.
M_H = 10GeV(···), 100 GeV (—), 1000 GeV (- - -).
The single (full) curve corresponds to m_t = 230GeV, the others to m_t = 50GeV.

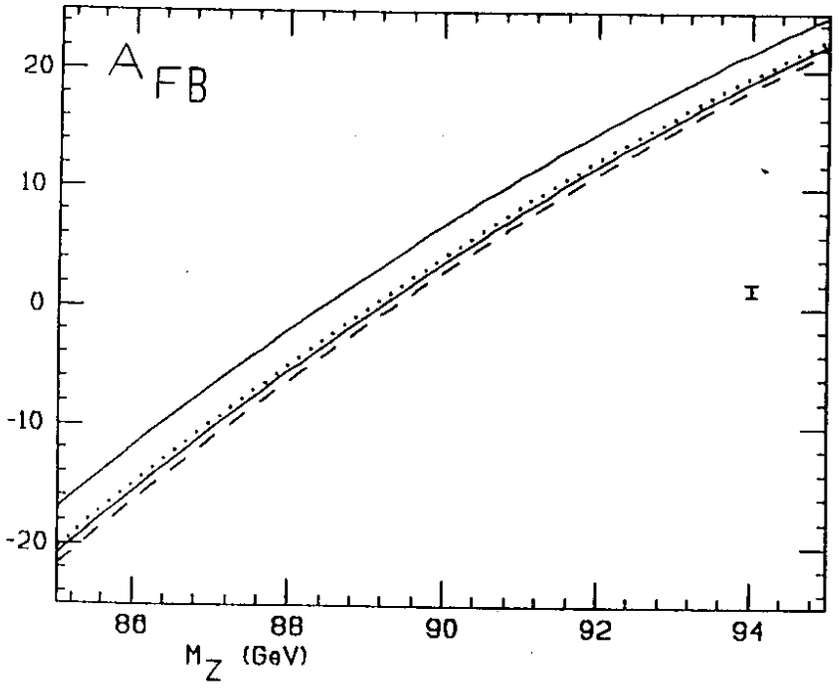

Figure 7:
A_{FB} for $e^+e^- \to b\bar{b}$ in %, $s = M_Z^2$.
Signature as in Figure 6

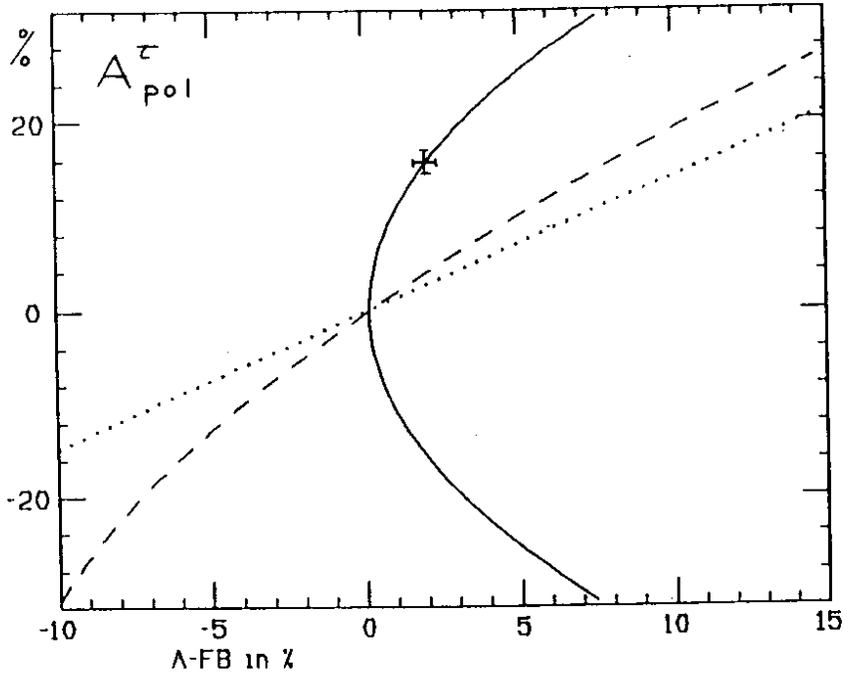

Figure 8:
τ-polarization A^{τ}_{pol} versus forward-backward asymmetries A_{FB} for $e^+e^- \to f\bar{f}$ muons (———), c-quarks (- - -), b-quarks (···). $s = M_Z^2$.

term mentioned above has been switched off since it is not incorporated in the Dubna-Zeuthen calculation. [1] An agreement within 0.2% has been obtained also for the angular distributions in quark pair production (tables 5 and 6)

θ	$\sqrt{s}$ =89	93 GeV	97 GeV
30°	0.01196	0.20881	0.03121
	0.01196	0.20883	0.03118
90°	0.01158	0.11353	0.01228
	0.01157	0.11356	0.01227
150°	0.02858	0.18855	0.01177
	0.02855	0.18863	0.01178

Table 4a

θ	$\sqrt{s}$ =89	93 GeV	97 GeV
30°	0.01271	0.21231	0.03223
	0.01272	0.21236	0.03221
90°	0.01190	0.11400	0.01264
	0.01189	0.11401	0.01264
150°	0.02893	0.18670	0.01201
	0.02890	0.18666	0.01201

Table 4b

Differential cross section for $e^+e^- \to \mu^+\mu^-$ in nbarn.
upper values: based on [19]; lower values: based on [12,20]
M_Z = 93 GeV, M_H = 100 GeV, α_s = 0.12
a: m_t = 60 GeV; b: m_t = 200 GeV.

[1] see also "Electroweak Radiative Corrections". For muons this term is not significant; for d-type quarks it matches the experimental accuracy for top masses around 200 GeV. It is incorporated in figures 6 and 7.

θ	$\sqrt{s}$ =89	93 GeV	97 GeV
30°	0.06530	0.84997	0.11017
	0.06535	0.85021	0.11008
90°	0.04104	0.41057	0.04460
	0.04102	0.41056	0.04458
150°	0.07833	0.58701	0.04593
	0.07820	0.58674	0.04594

Table 5:
Differential cross section for $e^+e^- \to u\bar{u}$.
upper values: based on [19]; lower values: based on [12,20]
M_Z = 93 GeV, M_H = 100 GeV, m_t = 200 GeV, α_s = 0.12

θ	$\sqrt{s}$ =89	93 GeV	97 GeV
30°	0.10276	1.1407	0.13059
	0.10285	1.1411	0.13047
90°	0.05171	0.52441	0.05594
	0.05168	0.52438	0.05591
150°	0.07822	0.69472	0.06519
	0.07804	0.69423	0.06521

Table 6:
Differential cross section for $e^+e^- \to d\bar{d}$ in nbarn.
upper values: based on [19]; lower values: based on [12,20]
M_Z = 93 GeV, M_H = 100 GeV, m_t = 200 GeV, α_s = 0.12

Also for comparison, we show in table 7 the results on the integrated on-resonance muon asymmetry for various input parameters with restriction to $O(\alpha)$, as done in table 4. As one can see, the agreement is at least an order of magnitude better than the experimental uncertainty.

M_Z (GeV)	m_t (GeV)	$M_H = 10$	100	1000 GeV
90	50	0.0044	0.0037	0.0027
		0.0043	0.0036	0.0027
	100	0.0051	0.0044	0.0036
		0.0051	0.0044	0.0036
	150	0.0058	0.0050	0.0043
		0.0057	0.0050	0.0043
	200	0.0061	0.0053	0.0048
		0.0061	0.0054	0.0048
	230	0.0059	0.0051	0.0047
		0.0060	0.0052	0.0048
91	50	0.0124	0.0111	0.0092
		0.0124	0.0111	0.0091
	100	0.0141	0.0128	0.0110
		0.0140	0.0127	0.0109
	150	0.0158	0.0145	0.0129
		0.0158	0.0145	0.0129
	200	0.0176	0.0163	0.0148
		0.0177	0.0164	0.0149
	230	0.0185	0.0171	0.0159
		0.0187	0.0173	0.0160
92	50	0.0248	0.0229	0.0203
		0.0247	0.0228	0.0201
	100	0.0272	0.0253	0.0228
		0.0271	0.0253	0.0227
	150	0.0299	0.0280	0.0256
		0.0299	0.0280	0.0256
	200	0.0329	0.0310	0.0289
		0.0330	0.0311	0.0289
	230	0.0346	0.0328	0.0308
		0.0349	0.0330	0.0310

Table 7:
A_{FB} for $e^+e^- \to \mu^+\mu^-$, $s = M_Z^2$
upper values: based on [19]; lower values: based on [12,20].

5 $O(\alpha)$ QED corrections to A_{FB}

5.1 General features

The common distinguishing feature of the weak corrections discussed so far is their independence of the experimental set-up. The $O(\alpha)$ QED corrections (real and virtual single photon contributions) are the result of an incoherent superposition of 2-particle and (inclusive) 3-particle final states. The bremsstrahlung cross section, differential with respect to the outgoing fermion, is obtained by integrating the radiated photon over the allowed phase space:

$$\frac{d\sigma^B}{d\Omega_f} = \int \frac{d\sigma}{d\Omega_f\, d\Omega_\gamma\, dE_\gamma} dE_\gamma d\Omega_\gamma \,. \tag{22}$$

This phase space can either be the entire one obeying only the kinematical bounds, or it can be restricted by additional cuts according to the requirements of a specific experiment. In order to obtain an infra-red finite result it is sufficient to deal with the soft photon part of the real bremsstrahlung cross section. The soft photon approximation means that the radiated photon energy $k^0 \leq \Delta E$ is restricted to a maximum energy ΔE which is small compared to the energy of the scattering process: $\Delta E \ll \sqrt{s} = 2E$. Since the photons radiated from the initial state need not necessarily be soft with respect to the resonance width, however, the energy loss in the Z propagator has to be taken into account in the Z propagator.

In real experiments the restriction to small values of $\Delta E/E$ is often not applicable due to the geometrical layout of a realistic detector. Then also hard photons with $k^0 > \Delta E$ become important and the definition of the final state may depend on other restrictions like accollinearity cuts to the outgoing fermions. The proper hard photon part is IR and UV finite; it can be treated as decoupled from the rest of the electroweak cross section. The electroweak properties of the Z boson enter only globally in terms of the characterizing quantities mass, width, and coupling constants. For the adaptation between the soft and hard part it has to be ensured that they are consistent with each other.

In order to set up a common terminology we refer to the following classification (note that each subclass is gauge invariant by itself and hence allows a separate treatment; this is of particular importance since they show also different qualitative and quantitative behaviour):

initial state corrections:

real photons

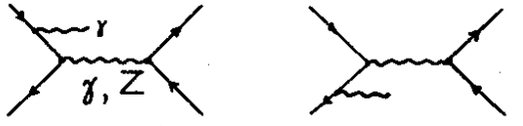

virtual photons

final state corrections:

real photons

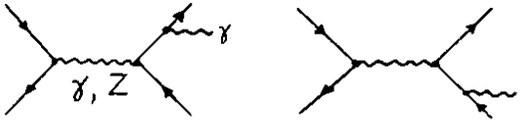

virtual photons

initial-final state interference corrections:

real photons

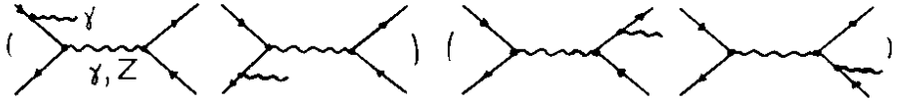

virtual photons

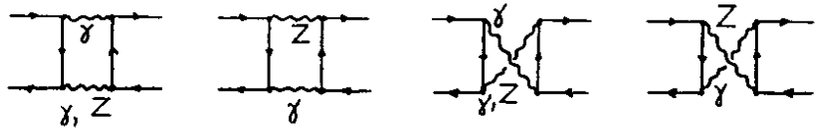

The initial and final state corrections are functions of s only; the interference contributions depend in addition also on the scattering angle and induce a modification of the θ dependence of the differential cross section. Their actual magnitude depends crucially on the applied cuts (see the discussion below in section 5.3).

5.2 Inventory of the present situation

The complete $O(\alpha)$ corrections have been caclulated by various authors: Berends, Kleiss, Jadach [3]; Böhm, Hollik [4]; Bardin et al. [13]; the soft photon part also by Greco et al. [2] (obtained from their exponentiated formulae by expansion to $O(\alpha)$). The references [2,3,4] utilize as global input only the parameters M_Z, Γ_Z, s^2_W; [13] includes also the full weak corrections where the parameters are interrelated via the G_μ constraint (13). This has also been done by Berends, Kleiss, Hollik [21]. Furthermore, there is an independent calculation (also with full weak corrections) by Igarashi et al. [10] where M_W and M_Z are independent input parameters (no G_μ constraint applied).

Most of the hard photon calculations are done by Monte Carlo methods [3,10,14,21]. Only [13] is an analytic integration also of the hard photon part, complete to $O(\alpha)$. Analytic calculations are appreciated as a reference for Monte Carlo programs. Whereas MC's allow all kinds of experimental restrictions, the calculation [13] yields the differential cross section as well as the integrated quantities σ, A_{FB} section for a situation

where no cuts have been applied to the emitted photon. Meanwhile there is also a version which allows cuts to the photon energy resp. to the invariant mass of the outgoing fermion pair [22].

Before this Workshop a numerical comparison between the results of different authors was difficult because of the non-standardized "Born-like" input (which means everything without the extra real or virtual photon) in the radiative amplitudes.

The parametrization of the lowest order cross section in terms of the vector and axial vector coupling constants $v_{e,f}$, $a_{e,f}$ as given in section 2, eqs. (6) and (7), is quite general and applies to any model where a vector boson with v and a couplings is exchanged together with the photon. Expressing also the radiative amplitudes resp. the bremsstrahlung cross section (22) in terms of these global parameters is also free of ambiguities as far as the parameters are kept as free input quantities.

In the Standard Model, however, these quantities are not independent. For a quantitative evaluation a well-known ambiguity in the Born level presentation shows up: the coupling constants can either be expressed by means of (4), or, utilizing (13) without the correction Δr, by

$$\begin{aligned} a_f &\rightarrow \left(\frac{\sqrt{2}G_\mu M_Z^2}{4\pi\alpha}\right)^{1/2} I_3^f \\ v_f &\rightarrow \left(\frac{\sqrt{2}G_\mu M_Z^2}{4\pi\alpha}\right)^{1/2} (I_3^f - 2\,Q_f\,s^2_W)\,. \end{aligned} \tag{23}$$

The numerical results obtained for A^0_{FB} from these two parametrizations are different in general. Of course, after incorporating consistently the weak radiative corrections described in the previous section, we obtain an unambigous answer for the result without QED corrections. Another way of presenting the amplitudes dressed by non-QED corrections is the use of effective coupling constants around the Z (see the "Electroweak Radiative Corrections"contribution) in terms of (complex) correction factors ρ_f and κ_f for each fermion species:

$$\begin{aligned} a_f &\rightarrow \left(\frac{\sqrt{2}G_\mu M_Z^2}{4\pi\alpha}\,\rho_f\right)^{1/2} I_3^f \\ v_f &\rightarrow \left(\frac{\sqrt{2}G_\mu M_Z^2}{4\pi\alpha}\,\rho_f\right)^{1/2} (I_3^f - 2\,Q_f\,\kappa_f\,s^2_W)\,, \end{aligned} \tag{24}$$

together with s^2_W derived from (13). For not too large top masses ($m_t < 130$ GeV) ρ_f and κ_f differ only little from 1, which means that the parametrization (23) is a good "Born-like" input for the calculation of the bremsstrahlung cross section (together with the physical width in the Z propagator). Since the Z exchange in the parametrization (23) does not get large corrections from the photon vacuum polarization [2] a consensus was achieved that the input quantities M_Z, Γ_Z, s^2_W, together with (23), should be used for comparisons of the numerical results for the QED corrected asymmetries. This strategy has been used for the $O(\alpha)$ as well as for the higher order QED corrections of the following sections.

[2] see section 4.1, in particular the cancellation of $\Pi_{\gamma\gamma}$ between Δr and Π_Z.

After the consensus on a standard input it has become possible to obtain numerical agreement in the results for the complete $O(\alpha)$ corrections and also for the leading higher order contributions within the required accuracy.

5.3 Discussion of the various contributions

5.3.1 Final state corrections

The final state corrections are similar to the situation encountered also in the off-resonance region:
According to our general presentation (1) of A_{FB} as the ratio of the antisymmetric to the symmetric part of the cross section the effects can be summmarized as follows:

If **no cuts** are applied, only the symmetric part

$$\sigma = \sigma_F + \sigma_B$$

gets a correction:

$$\sigma \to \sigma \cdot \left(1 + \frac{3\alpha}{4\pi} Q_f^2\right) \tag{25}$$

whereas

$$\delta(\sigma_F - \sigma_B) = 0\,. \tag{26}$$

This results in a correction to the asymmetry

$$A_{FB} \to A_{FB} \cdot \left(1 - \frac{3\alpha}{4\pi} Q_f^2\right) \tag{27}$$

which is a very small negative contribution (< 0.17 % relative to A_{FB}).

These final state corrections have first been calculated for the QCD single gluon emission [23], leading to the following asymmetry for quark final states:

$$A_{FB} \to A_{FB} \cdot \left(1 - \frac{\alpha_s}{\pi}\right) \tag{28}$$

with quark masses $\ll M_Z$. This has been confirmed by Djouadi [24] for the QCD case. When translated to QED, the above result in (27) is obtained. Independently, this result has been obtained also in the direct QED calculation by Bardin et al [13].

For massive quarks, the QCD final state corrections can be included by multiplying the purely electroweak asymmetry by a factor

$$1 - \frac{\alpha_s}{\pi} \Delta_q\,.$$

The coefficient Δ_q is, to a very good approximation (1%) for the known quarks given by

$$\Delta_q = 1 - \frac{4}{3}\pi \frac{m_q}{M_Z} \tag{29}$$

which means that

$$\Delta_q = \begin{cases} 1 & \text{for } u,d\text{-quarks} \\ 1 - 0.02 & \text{for } s\text{-quarks} \\ 1 - 0.07 & \text{for } c\text{-quarks} \\ 1 - 0.21 & \text{for } b\text{-quarks} \end{cases} \tag{30}$$

with $m_s = 500$ MeV, $m_c = 1.5$ GeV, $m_b = 4.5$ GeV, $M_Z = 91$ GeV, and $\alpha_s = 0.11$. The exact formulae are given in the report of the "Heavy Quarks" group together with some expressions for "2-jet asymmetries ".

More **restrictive** cuts with $E_\gamma < \Delta E \ll E = \sqrt{s}/2$ (soft photon domain) yield larger corrections to the cross section but multiply the symmetric and antisymmetric part in the same way [2,3,4]:

$$(\sigma_F \pm \sigma_B) \cdot \left[1 + \frac{2\alpha}{\pi} Q_f^2 \beta_f \log\frac{\Delta E}{E} + \frac{3\alpha}{2\pi} Q_f^2 \beta_f + \frac{\alpha}{\pi} Q_f^2 \left(\frac{\pi^2}{3} - \frac{1}{2}\right)\right] \tag{31}$$

with

$$\beta_f = \log\frac{s}{m_f^2} - 1\,.$$

These corrections therefore cancel in the asymmetry (1):

$$\delta(A_{FB}) = 0\,. \tag{32}$$

This remains valid also after the soft photon contributions have been summed to all orders as done by Greco et al.[2] (see also section 6).

In general, with or without cuts, the asymmetry is affected only very little by the final state corrections.

5.3.2 Initial - final state interference:

In the interference contributions no large logarithms $\log(s/m_f^2)$ are present; instead, angular dependent terms like

$$\log\frac{t}{u} = \log\frac{1 - \cos\theta}{1 + \cos\theta}$$

enter the result, which induce an additional asymmetry. In the Z region the resonant diagrams

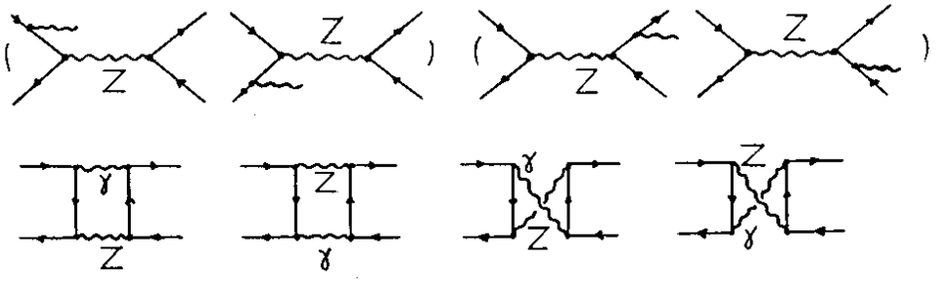

are the most important ones; the others are associated with the photon exchange and hence are suppressed by an additional factor Γ_Z/M_Z.

In the resonance region the interference contributions show a behaviour different from the continuum and can be easily understood in terms of the resulting correction factor (from the diagrams listed above) [2,3,4] for the angular distribution close to the peak:

$$1 + Q_e Q_f \left\{ \frac{4\alpha}{\pi} \log \frac{t}{u} \log \mid \epsilon \frac{s}{M_R^2 - s + s\epsilon} \mid + X^B_{fin}(\theta) + V^{\gamma Z}_{fin}(\theta) \right\} \equiv 1 + C_{int}(\theta) \qquad (33)$$

with

$$\epsilon = \frac{\Delta E}{E} = \frac{2\Delta E}{\sqrt{s}}, \quad M_R^2 = M_Z^2 - iM_Z\Gamma_Z \,,$$

which is antisymmetric and multiplies the symmetric part of the resonant angular distribution, yielding

$$\delta(\sigma_F - \sigma_B) = \frac{\alpha^2}{4s} \cdot 2 \int_0^1 d\cos\theta \, (v_e^2 + a_e^2)(v_f^2 + a_f^2) \mid \chi \mid^2 \cdot (1 + \cos^2\theta) \cdot C_{int}(\theta) \qquad (34)$$

$$\simeq \frac{\alpha^2}{4s} \cdot (v_e^2 + a_e^2)(v_f^2 + a_f^2) \mid \chi \mid^2 \cdot \frac{2\alpha}{\pi} Q_e Q_f (1 + 8\log 2) \log \mid \frac{M_R^2 - s + s\epsilon}{s\epsilon} \mid .$$

X^B_{fin} denotes the finite (non-IR) part of the real photon and $V^{\gamma Z}_{fin}$ that of the virtual photon contributions. For $s \approx M_Z^2$ the finite virtual term has the property [3]

$$V^{\gamma Z}_{fin}(\theta) \; = \; -X^B_{fin}(\theta) \; + \; O\left(\frac{\alpha}{\pi}\frac{\Gamma_Z}{M_Z}\right) ; \qquad (35)$$

consequently, the log-term in (33) is practically the only part responsible for an additional antisymmetric contribution. Its size depends crucially on the cuts applied to the radiated photon:
(i) For very loose cuts ($\epsilon \to 1$) this term becomes also of order $O\left(\frac{\alpha}{\pi}\frac{\Gamma_Z}{M_Z}\right)$ which means that the total contribution to the asymmetry is negligibly small. This corresponds exactly to the situation of a very narrow resonance [25] where the interference contributions are practically zero.
(ii) For tight cuts ($\epsilon \approx 0.01$) this log term yields a positive contribution of a few percent to the asymmetry.

The above consideration is based on the formulae valid for soft photons. The proper inclusion of hard photons for the case (i) does not change the result that the interference contribution is negligible [13,15]. This is substantiated in figure 9 where the interference contribution to the muon A_{FB} is shown as function of the maximum photon energy. For cuts $\epsilon > 10^{-1}$ the interference contributes less than 0.001 to A_{FB}. Note that δA^*_{FB} in figure 9 and in [15] is defined as the first moment of $\cos\theta$ which deviates for hard photons from the conventional definition. The dotted curve in figure 9 is the result for the conventional asymmetry as obtained from the soft photon expression (34), where the $O\left(\frac{\alpha}{\pi}\frac{\Gamma_Z}{M_Z}\right)$ terms have been neglected. In both cases the symmetric cross section in the denominator of A_{FB} includes the single photon contributions for the same cuts. The comparison shows that for those cuts where the interference contributions become sizeable our simple formula already gives a reasonable approximation. The black dots

[3] for the complete expression see e.g. [19].

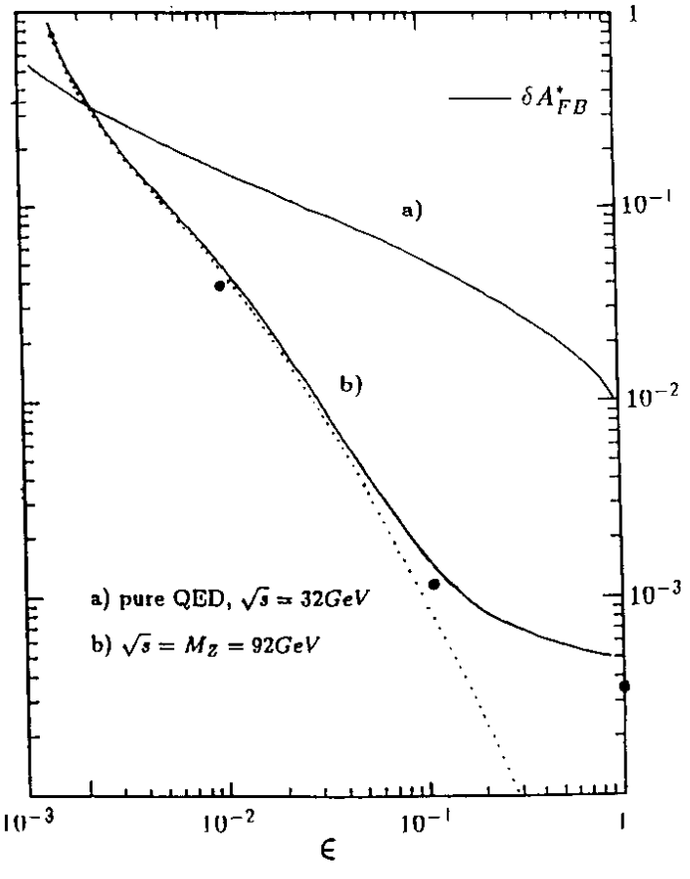

Figure 9:
The interference contribution to A_{FB}, versus $\epsilon = \Delta E/E$
$\cdots$ soft-photon approximation; • Dubna-Zeuthen results.
—— non-conventional definition of A_{FB} as moment of $\cos\theta$.
Curve a) illustrates the interference contribution well below the resonance.

indicate the results for the conventional A_{FB} with hard photons as obtained by the Dubna-Zeuthen collaboration. The purpose of this plot is to show the increase of the interference contribution with decreasing ϵ; for a quantitative discussion at very low values, however, the higher order contributions beyond $O(\alpha)$ become also of importance and have to be included. For practical situations with not very severe cuts, the interference term is under control. For quark final states, the corresponding δA_{FB} from the interference is even smaller due to the charge factors.

5.3.3 Initial state corrections

As is well known for the integrated cross section [see the 'Z line shape' contribution] the $O(\alpha)$ initial state corrections give rise to a 40 % reduction of the peak height. This is due to the rapid variation of $\sigma(s)$ with the energy. Since the asymmetry $A_{FB}(s)$ is a steeply increasing function around the Z the energy loss from initial-state radiation $s \to s' < s$ leads to a reduction in the asymmetry as well:

$$A_{FB}(s') < A_{FB}(s)\,.$$

Quantitatively, the correction to A_{FB} close to the peak is given by

$$\delta A_{FB} \simeq -0.025$$

which is of the order of the on-resonance asymmetry itself. From this behaviour it is clear that for a realistic treatment also the higher order QED contributions have to be investigated carefully. This will be done in the next section.

In $O(\alpha)$, the exact analytic calculations are available [13,26]. This allows us to express the initial state QED corrections to A_{FB} in a compact form, quite in analogy to the convolution integral for the integrated cross section:

$$A_{FB}(s) = \frac{1}{\sigma_T(s)} \int_{z_0}^{1} dz\, \frac{4z}{(1+z)^2}\, \tilde{H}_e^{(1)}(z)\, \sigma_{FB}^0(zs)\,, \qquad z_0 \geq \frac{4m_f^2}{s}\,. \tag{36}$$

The basic ingredients are the Born expressions (see eqs (1),(2) and (6),(7) of section 2) for [4]

$$\sigma_{FB}^0(s) \equiv \sigma_F^0(s) - \sigma_B^0(s) = \frac{\pi\alpha^2}{s} \cdot G_3(s)$$

(massless fermion approximation) and the distribution function

$$\begin{aligned} \tilde{H}_e^{(1)}(z) &= \delta(1-z) \\ &+ \frac{\alpha}{\pi}\left\{\delta(1-z)\left[(2\log\epsilon + \frac{3}{2})(L_e - 1) + \frac{\pi^2}{3} - \frac{1}{2}\right]\right. \\ &+ \left.\theta(1-\epsilon-z)\,\frac{1+z^2}{1-z}\left[L_e - 1 - \log\frac{4z}{(1+z)^2}\right]\right\} \end{aligned} \tag{37}$$

[4] $\sigma_{F,B}^0$ can be calculated with the coupling constants (4) or (23) (see section 5.2), or with inclusion of the non-QED corrections in order to give the complete 1-loop result. For the purpose of studying the QED corrections we restrict the discussion here to the Born couplings without weak dressing.

where

$$s' = zs = (p_f + p_{\bar{f}})^2$$

is the invariant mass of the outgoing fermion pair and

$$L_e = \log\frac{s}{m_e^2}\,. \tag{38}$$

The form (36) together with the leading logarithmic terms $\sim \frac{\alpha}{\pi} L_e$ from (37) (as well as the next order $(\frac{\alpha}{\pi} L_e)^2$ contribution, see next section) has also been derived by Beenakker et al. [27] applying renormalization group methods.

The distribution $\tilde{H}_e^{(1)}(z)$ for the antisymmetric cross section in (36)

$$\tilde{H}_e^{(1)}(z) = H_e^{(1)}(z) - \theta(1-\epsilon-z)\,\frac{\alpha}{\pi}\,\frac{1+z^2}{1-z}\,\log\frac{4z}{(1+z)^2} \tag{39}$$

contains a part $H_e^{(1)}(z)$ which enters the total cross section:

$$\sigma_T(s) = \int_{z_0}^{1} dz\, H_e^{(1)}(z)\, \sigma_T^0(zs) \tag{40}$$

with the Born term (massless fermion approximation)

$$\sigma_T^0(s) = \frac{4\pi\alpha^2}{3s} \cdot G_1(s)$$

according to eq. (6).

It is not surprising that the convolution kernel for the antisymmetric part of the cross is different from that for the symmetric one, since σ_{FB} is a less inclusive quantity than σ_T and the kinematical situation is more complicated. In several practical applications [28,29,30] the exact form (36) has been approximated by the simpler expression

$$A_{FB}(s) \simeq \frac{1}{\sigma_T(s)} \int_{z_0}^{1} dz\, H_e^{(1)}(z)\, \sigma_{FB}^0(zs) \tag{41}$$

with the same weight $H_e^{(1)}(z)$ (the "radiator") as in the total cross section (40). It is valid for soft photons and in the collinear leading logarithmic approximation provided the scattering angle is used in the rest frame of the outgoing $f\bar{f}$ pair. This angle is in general different from the laboratory scattering angle θ in terms of which the expression (36) has been derived (conventional definition of A_{FB}). Close to the Z resonance, however, these differences are small and (41) can be applied to calculate A_{FB} as defined in the conventional way as well. The differences between (36) and (41) occur only in the hard photon region ($z \to 0$) and disappear for soft photons where $4z/(1+z)^2 \to 1$. Close to the Z peak, however, soft photons are dominant since hard photon emission leads off the resonance peak. Hence, these left-out hard photon effects are not of importance for the Z asymmetries. Away from the resonance, where there is no hard photon suppression, (41) becomes insufficient and has to be replaced by the correct expression (36) together with (37).

An approach settled between (36) and (41) has been performed in [31]. The effect of the change in the scattering angle by the boost from the $f\bar{f}$–cms to the laboratory

frame is taken into account by the kinematical factor $4z/(1+z)^2$ in the convolution integral, but the symmetric weight function $H_e^{(1)}(z)$ from the total cross section is used:

$$A_{FB}(s) = \frac{1}{\sigma_T(s)} \int_{z_0}^{1} dz \, \frac{4z}{(1+z)^2} H_e^{(1)}(z) \, \sigma_{FB}^0(zs). \tag{42}$$

Since the difference (39) between $H_e^{(1)}$ and $\tilde{H}_e^{(1)}$ is of hard photon origin the replacement is not of practical importance at the Z.

The exact $O(\alpha)$ result is compared with the approximate calculation of A_{FB} from (41) in table 8 (see also ref [30]) for three energies close to the peak.

asymmetry	$M_Z - 5$ GeV	M_Z	$M_Z + 5$ GeV
A_{FB}^{Born}	-.4225	0.0207	0.4028
A_{FB}, approx	-.4242	-.0056	0.1860
A_{FB}, exact	-.4226	-.0055	0.1868

Table 8:
The $O(\alpha)$ initial state QED corrections to the muon A_{FB} without cuts.
$M_Z = 92.6$ GeV, $s_W^2 = 0.229$, $\Gamma_Z = 2.6$ GeV

6 Higher order QED corrections

A realistic treatment of A_{FB} requires the inclusion of QED corrections in higher than one-loop order. In general, the practical methods of dealing with higher order QED effects can be grouped as follows:
(i) soft photon resummation in the $O(\alpha)$ result
(ii) explicit 2-loop calculations
(iii) the structure function approach
(iv) multi-photon radiation according to the Yennie-Frautschi-Suura (YFS) formalism [32].

- (i) has been applied by the Dubna-Zeuthen group [26] improving the exact first order result in (36),(37) by taking into account the IR soft photons to all orders in the convolution integral.
- (ii) has been done by Berends et al. [33] for the integrated cross section performing the explicit calculation of the 2-loop diagrams contributing to the initial state corrections, together with the resummation of soft photons to all orders. For the asymmetry, the leading logarithmic terms have been derived to $O(\alpha^2)$ [27] and the soft photon contributions have also been resummed.
- (iii) has been applied to the integrated cross section by Nicrosini, Trentadue [34] and Campagne, Zitoun [35], also with final state radiation and soft photon resummation. The formalism has been applied to A_{FB} in the approximation that the $O(\alpha^2)$ kernels are taken over from the symmetric cross section. For the initial state radiation this has also been done by Jadach and Wąs [28].

- (iv) has been implemented in a MC program by Jadach and Ward [36] in order to generate final states with multiple soft (IR) photons to all orders and hard photons up to $O(\alpha^2)$.

For the most important case of initial-state radiation we want to discuss the approaches (i) - (iii) for A_{FB} in some more detail. They have in common that they allow a compact representation and are formally equivalent to the convolution type expressions given in section 5.3.3 where only the kernels have to be modified according to the inclusion of the higher order contributions.

Case (i):

The inclusion of the soft photon contribution to all orders in the $O(\alpha)$ result is done by replacing the convolution kernel of (36) with $\tilde{H}_e^{(1)}$ from (37) in the following way:

$$\begin{aligned} \frac{4z}{(1+z)^2}\tilde{H}_e^{(1)}(z) \;\to\; & \frac{2\alpha}{\pi}(L_e-1)(1-z)^{\frac{2\alpha}{\pi}(L_e-1)-1}\left\{1+\frac{\alpha}{\pi}\left(\frac{3}{2}(L_e-1)+\frac{\pi^2}{3}-\frac{1}{2}\right)\right\} \\ & + \frac{\alpha}{\pi}\left\{\left(\frac{4z}{(1+z)^2}\frac{1+z^2}{1-z}-\frac{2}{1-z}\right)(L_e-1)-\frac{4z}{(1+z)^2}\log\frac{4z}{(1+z)^2}\right\}. \end{aligned} \tag{43}$$

Case (ii):

In the leading log (LL) approximation up to second order the formula (36) is valid with the following distribution function replacing $\tilde{H}_e^{(1)}$:

$$\tilde{H}_e^{(2)LL}(z) = H_e^{(2)LL}(z) + h_e^{(2)LL}(z) \tag{44}$$

where

$$\begin{aligned} H_e^{(2)LL}(z) = \; & \delta(1-z) + \frac{\alpha}{\pi}L_e\left\{\delta(1-z)(2\log\epsilon+\frac{3}{2}) + \theta(1-\epsilon-z)\frac{1+z^2}{1-z}\right\} \\ & + \left(\frac{\alpha}{\pi}L_e\right)^2\left\{[\delta(1-z)\left[2\log^2\epsilon+3\log\epsilon+\frac{9}{8}-2\zeta(2)\right]\right. \\ & \left. + \theta(1-\epsilon-z)\left[\frac{1+z^2}{1-z}(2\log(1-z)-\log z+\frac{3}{2})+\frac{1+z}{2}\log z-(1-z)\right]\right\} \end{aligned} \tag{45}$$

is the LL $O(\alpha^2)$ radiator for the total cross section (40), and $h_e^{(2)LL}$ denotes the difference to the antisymmetric kernel appearing in the LL approximation in second order:

$$\begin{aligned} h_e^{(2)LL}(z) = \; & \left(\frac{\alpha}{2\pi}L_e\right)^2 \cdot \\ & \cdot\left[\frac{(1-z)^3}{2z}+\frac{(1-z)^2}{\sqrt{z}}(\arctan\frac{1}{\sqrt{z}}-\arctan\sqrt{z})-(1+z)\log z+2(1-z)\right]. \end{aligned} \tag{46}$$

This term contributes only for hard photons.

The soft photon resummation to all orders can be performed by the following replacement:

$$\tilde{H}_e^{(2)LL} \to \tilde{H}_e^{LL} = H_e^{LL} + h_e^{(2)LL} \tag{47}$$

with

$$H_e^{LL}(z) = \frac{2\alpha}{\pi} L_e (1-z)^{\frac{2\alpha}{\pi}L_e - 1} \left[1 + \frac{\alpha}{\pi} L_e \cdot \frac{3}{2} + \left(\frac{\alpha}{\pi} L_e\right)^2 \left(\frac{9}{8} - 2\zeta(2)\right) \right] \qquad (48)$$
$$- \frac{\alpha}{\pi} L_e (1+z) + \left(\frac{\alpha}{\pi} L_e\right)^2 \cdot$$
$$\cdot \left[-\frac{1+z^2}{1-z} \log z + \frac{1+z}{2} \log z - 2(1+z)\log(1-z) - (1-z) - \frac{3}{2}(1+z) \right]$$

and $h_e^{(2)LL}$ from (46).

Case (iii):

The structure function approaches of [28] and [29] take the simplified approximate convolution formula (41) for calculating A_{FB} with the help of the same higher order weight function with soft photon resummation for the total cross section. We do not list them here since they are given in the "Z line shape" contribution to this report and in the corresponding literature. The weight function for the symmetric cross section [35] is also used by Campagne and Zitoun [31], but in the convolution integral (42) instead of (41). For the question of cuts to the outgoing fermion pair we refer to the Monte Carlo part of this report.

In table 9 we put together the results of the various groups for the $e^+e^- \to \mu^+\mu^-$ asymmetry. They have been obtained with the following conventions:
- Born formulae of section 2 for $\sigma^0_{F,B}$ with $\mu_f = 0$,
- parametrization (23) for the coupling constants v_f, a_f,
- numerical values $M_Z = 93$ GeV, $\Gamma_Z = 2.5$ GeV, $s^2_W = 0.23$ for the input quantities.

As one can see from table 9, the QED contributions in higher than $O(\alpha)$ give rise to a shift of the on-resonance asymmetry from -0.4% to $+0.3\%$ which is twice as much as the experimental uncertainty. The last 4 lines contain the $O(\alpha^2)$ corrections together with the soft photon resummation and are therefore the "best" values presently available for the given Born input. The comparison of the results in these lines shows that there is good agreement between the various approaches: within $0.5 \cdot 10^{-3}$ close to the peak, at $s = M_Z^2$ within $0.3 \cdot 10^{-3}$. One can also see that the $O(\alpha)$ corrections with soft photon resummation already give satisfactory predictions, within the small deviations between the other results. Away from the resonance peak the differences between the various groups become larger: 0.009 below and 0.018 above the resonance.

Jadach and Wąs [28] have investigated also several variants for definitions of A_{FB} with the help of multi-photon (initial state) Monte Carlo [36] simulation. All the asymmetries which differ in the hard photon domain agree within negligibly small deviations ($< 0.6 \cdot 10^{-3}$) close to the Z. This confirms again that hard photon terms are not of importance.

Final state radiation does not give a significant modification of A_{FB} unless severe cuts are imposed, as discussed in section 5.3.2. It has been incorporated in the compact convolution formula for A_{FB} of the type (41) in the following way [29]:

$$A_{FB}(s) = \int_{z_0}^{1} dz\, H_e(z)\, F_f(1 - z_0 - z, zs)\, \sigma^0_{FB}(zs). \qquad (49)$$

$\sqrt{(s)}$ (GeV)	82	92.5	93	93.5	100
Born	-69.99	-2.221	1.887	5.923	47.28
Dubna/Zeuthen, $O(\alpha)$ [13,26]	-53.08	-4.009	-0.403	2.920	19.36
Dubna/Zeuthen, $O(\alpha)$, resummed [26]	-54.63	-3.643	0.289	3.760	20.49
LL, $O(\alpha^2)$ [27]	-53.03	-3.548	0.352	3.749	18.51
LL, $O(\alpha^2)$, resummed [27]	-53.34	-3.638	0.293	3.762	18.85
Jadach/Wąs, resummed [28]	-54.20	-3.672	0.260	3.724	20.11
Montagna et al. , resummed [29]	53.96	-3.693	0.276	3.783	18.79
Campagne/Zitoun, resummed [31]	-53.95	-3.670	0.277	3.770	20.31

Table 9:
A_{FB} for $e^+e^- \to \mu^+\mu^-$ in % around the resonance with initial state QED corrections
$M_Z = 93$ GeV, $\Gamma_Z = 2.5$ GeV, $\sin^2\theta_W = 0.23$

The final state radiation function F_f is again taken from the case of the integrated symmetric cross section, explicitly given in [34] for $f = \mu$. In a similar way, Campagne and Zitoun have incorporated the final state radiation on the basis of the convolution formula (42) with the additional kinematical factor, but also with H_e, F_f as used for the total cross section [35]. For more details see the contribution "Compact formula" in the Monte Carlo part of this report.

A principle problem in all practical applications of the compact formalism with multi-photon radiation is the incorporation of the interference term. From the practical point of view, however, this term is negligible for not too tight cuts (see the discussion in 5.3.2). For tight cuts where the soft-photon approximation is applicable, Greco et al. [2] have given a prescription how to treat the interference contribution in higher orders. In the structure function approach of [29] and [31] the interference terms is added by hand in $O(\alpha)$ to the convolution integral. Numerically, for a cut to the radiated photon energy of $E_\gamma < 1$ GeV good agreement has been obtained with the results based on the formulae of [2]. For tighter cuts, however, the higher order contributions in the interference term become apparent. Figure 10 displays the situation with the cut $E_\gamma < 1$ GeV: the dashed curve contains initial and final state radiation without interference, and the full curve includes the $O(\alpha)$ interference term.

Figure 11 summarizes the situation where no cuts are applied. The behaviour of A_{FB} is qualitatively similar to that of the integrated cross section where the higher order QED contributions bring the prediction closer to the lowest order result than the $O(\alpha)$ corrections. The figure includes both initial and final state radiation with soft photon resummation and with the same conventions for the coupling constants (23) as in table 9. The effect of the final state radiation, however, is practically invisible.

All the numerical results of this section have been obtained with the constant width approximation in the Z propagator and with $\alpha = \alpha(0)$ normalizing the electromagnetic coupling strength in the photon exchange amplitude. In an improved Born approximation [see "Electroweak Radiative Corrections", section 4.6] one would replace the constant width term $M_Z\Gamma_Z$ by $s/M_Z\,\Gamma_Z$ in the Z and $\alpha(0)$ by $\alpha(M_Z^2)$ in the photon exchange. Whereas the effect of the s-dependent width is not significant ($\delta A_{FB} < 3\cdot 10^{-4}$) the rescaling of α yields a contribution of -0.002 for muons. After merging the QED corrections with the non-radiative, weakly dressed amplitudes of section 4, however, all these effects are automatically included consistently.

7 Conclusions

In this report we have given an overview of the evaluation of the forward-backward asymmetries in $e^+e^- \to f\bar{f}$ together with a description of the present status and have presented numerical results with checks on their reliability. In view of the experimental precision expected at the Z resonance peak our aim of getting a consensus on the theoretical numbers within $\Delta A_{FB} = \pm 0.001$ has been achieved, and noticeable differences, when they appear, are understood.

With the measured Z mass and the precisely known low energy parameters α, G_μ as

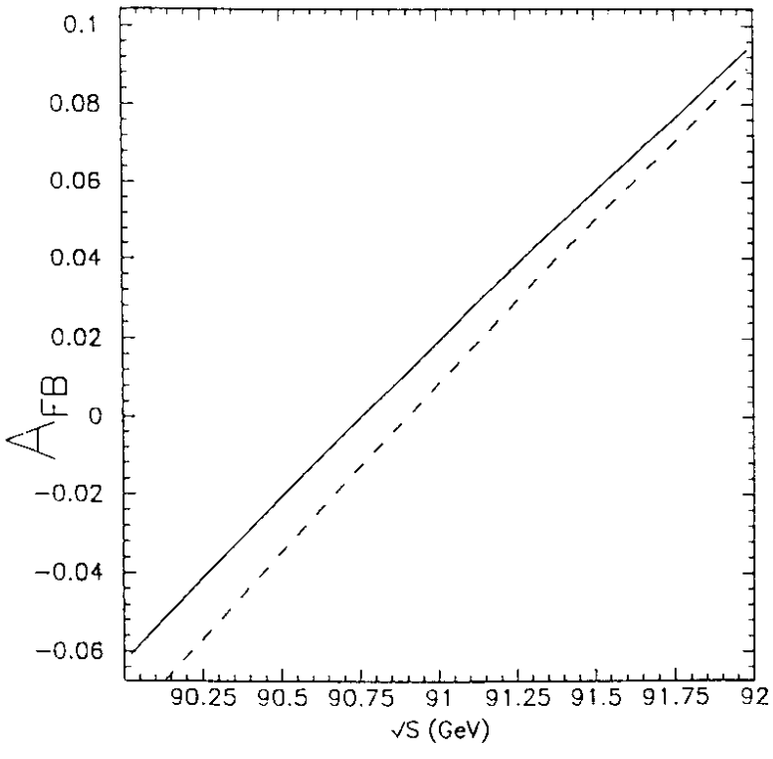

Figure 10:
A_{FB} for $e^+e^- \to \mu^+\mu^-$ for $E_\gamma < 1$ GeV.
Initial and final state radiation with soft photon resummation.
——— including interference, - - - - without interference
$M_Z = 91$ GeV, $\Gamma_Z = 2.47$ GeV, $\sin^2\theta_W = 0.232$

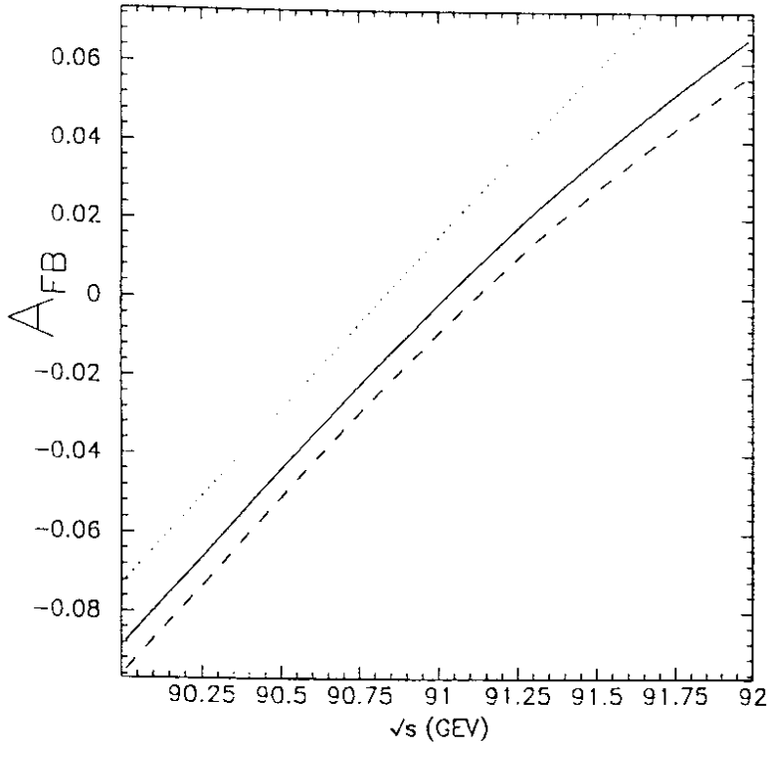

Figure 11:
A_{FB} for $e^+e^- \to \mu^+\mu^-$. Parameters as in Figure 10. No cuts.
$\cdots$ Born, - - - - $O(\alpha)$, —— $O(\alpha^2)$ and soft photon resummation

input quantities the asymmetries for the various final state fermions follow as predictions of the Standard Model. They depend in addition on the values of the Higgs and top mass which enter at the level of radiative corrections. Theradiative corrections have been split into two major subclasses according to their different qualitative features:

- the QED corrections:
  They are independent of the details of the underlying theory and need only the global parameters M_Z, Γ_Z, v_f, a_f in order to characterize the Z boson and its coupling constants. Due to their generality they apply to any kind of vector boson exchange with vector and axial vector couplings. Since they are large around the Z, the inclusion of higher than $O(\alpha)$ corrections is a necessity for reaching the required accuracy.

  Among the QED corrections, the most important contributions come from initial state radiation. The explicit calculation of the complete $O(\alpha)$ and leading $O(\alpha^2)$ corrections together with the resummation of soft photons to all orders is available. The results obtained for A_{FB} close to the peak agree within $5 \cdot 10^{-4}$ with those of other approaches which are different in non-leading and hard photon terms in $O(\alpha^2)$.

  The other QED corrections: final state radiation and initial-final interference, are negligibly small (below 0.001) if no tight cuts to the photon phase space are applied. These corrections are also available in analytical form, exact in $O(\alpha)$, and for the situation with cuts as well. More restrictive cuts make the interference contributions to A_{FB} important exceeding the level of 0.01 (for muons) when the photon is restricted to energies below 1 GeV. For very severe cuts (photon energy smaller than 1% of the incident electron energy) the higher order effects in the interference term also become significant. They exist in the soft photon approximation which is reasonable for these tight cuts. For realistic experiments, where the cuts are usually less severe, the $O(\alpha)$ term is sufficient. Compact analytical and semi-analytical formulae for the QED corrections have been derived and are available as FORTRAN programs [26,28,31]

- the genuine weak corrections:
  They correlate the global input parameters of the QED class via the underlying theory. In the Standard Model they allow us to predict the values of Γ_Z and the coupling constants in terms of α, G_μ, M_Z, M_H, m_t. Because of their model dependence it is sensible to treat them separately before merging with the QED corrections. The coupling constants which determine the asymmetries are effective couplings which get contributions from the vector boson self-energies, vertex corrections and box diagrams (the latter are negligible around the resonance). Two independent calculations have been compared at the one-loop level with the leading fermionic terms in the renormalization of α resummed to all orders: the agreement in the differential cross section at various energies and for various fermions is better than 0.2% and the integrated asymmetries agree within 0.0002 for top masses between 50 and 230 GeV and Higgs masses from 10 GeV to 1 TeV. When the $O(\alpha^2)$ leading term from a possibly heavy top quark is incorporated

[see "Electroweak Radiative Corrections"and ref,37 the predictions differ slightly for $m_t > 200$ GeV: for muons still negligible, and for d-type quarks matching the experimental accuracy.

The discussion and the obtained accuracy apply to leptonic and also to hadronic final states as far as the electroweak part is concerned. For $e^+e^- \to q\bar{q}$ the application of perturbative QCD yields an additional QCD correction to the quark asymmetries which is of about 4% (relative to the electroweak asymmetry) if no cuts to the hadronic final state are applied. The QCD factor depends slightly on the quark masses. For a more detailed discussion we refer to the "Heavy Flavor" contribution where also the questions of jet asymmetries and fragmentation will be covered.

References

1. G. Passarino and M. Veltman, Nucl. Phys. B 160 (1979) 151
2. M. Greco, G. Pancheri and Y. Srivastava, Nucl. Phys. B 171 (1980) 118; E: Nucl. Phys. B 197 (1982) 543
3. F.A. Berends, R. Kleiss and S. Jadach, Nucl. Phys. B 202 (1982) 63
4. M. Böhm and W. Hollik, Nucl. Phys. B 204 (1982) 45; Z. Phys. C 23 (1984) 31
5. W. Wetzel, Nucl. Phys. B 227 (1982) 1
6. M. Böhm and W. Hollik, Phys. Lett. 139 B (1984) 213
7. R.W. Brown, R. Decker and E.A. Paschos, Phys. Rev. Lett. 52 (1984) 1192
8. B.W. Lynn and R.G. Stuart, Nucl. Phys. B 253 (1985) 216
9. W. Hollik, Phys. Lett. 152 B (1985) 121
10. M. Igarashi, N. Nakazawa, T. Shimada and Y. Shimizu, Nucl. Phys. B 263 (1986) 347
11. M. Consoli and A. Sirlin, in: "Physics at LEP", CERN 86-02 (1986), eds. J. Ellis and R. Peccei, Vol. 1, p. 90
12. D. Yu. Bardin, P.Ch. Christova and O.M. Fedorenko, Nucl. Phys. B 197 (1982) 1
13. O.M. Fedorenko and T. Riemann, Acta Phys. Polon. B 18 (1987) 761; D.Yu. Bardin, M.S. Bilenky, O.M. Fedorenko, T. Riemann, Dubna Preprint JINR-E2-88-324 (1988)
14. D.C. Kennedy and B.W. Lynn, SLAC-PUB 4039 (1986, revised 1988); D.C. Kennedy, B.W.Lynn, C.J.C. Im and R.G. Stuart, SLAC-PUB-4128 (1988)
15. S. Jadach and Z. Wąs, Phys. Lett. B 219 (1989) 103
16. J. Drees, in: Proceedings of the Ringberg Workshop on "Radiative Corrections for e^+e^- Collisions", ed. J.H. Kühn, 1989; D. Treille, in "Polarization at LEP", CERN 88-06 (1988), eds. G. Alexander et al., Vol. 1, p. 265
17. A. Sirlin, Phys. Rev. D 22 (1980) 971
18. A.A. Akhundov, D.Yu. Bardin and T. Riemann, Nucl. Phys. B 276 (1986) 1; W. Beenakker and W. Hollik, Z. Phys. C 40 (1988) 141
19. W. Hollik, DESY 88-188 (1988), to appear in Fortschr. Phys.
20. D.Yu. Bardin, M. Bilenky, G. Mitselmakher, T. Riemann and M. Sachwitz, preprint Berlin-Zeuthen PHE 89-05 (1989), to appear in Z. Phys. C , and program ZBIZON

21. F.A. Berends, R. Kleiss and W. Hollik, Nucl. Phys. B 304 (1988) 712

22. D.Yu. Bardin, L. Vertogradov, Yu. Sedykh and T. Riemann, CERN-TH.5434/89 (1989), and program MUCUT

23. J. Jersak, E. Laerman and P.M. Zerwas, Phys. Rev. D 25 (1980)

24. A. Djouadi, Z. Phys. C 39 (1988) 561

25. M. Greco, G. Pancheri and Y. Srivastava, Nucl. Phys. B 101 (1975) 234; F.A. Berends and G.J. Komen, Nucl. Phys. B 115 (1976) 114

26. D.Yu. Bardin, M. Bilenky, A. Chizhov, A. Sazonov, Yu. Sedykh, T. Riemann and M. Sachwitz, CERN-TH.5411/89 (1989), and program MUCUT

27. W. Beenakker, F.A. Berends and W.L. van Neerven, in: Proceedings of the Ringberg Workshop on "Radiative Corrections for e^+e^- Collisions", ed. J.H. Kühn, 1989

28. S. Jadach and Z. Wąs, Preprint MPI-PAE/PTh 33/89, München 1989, and program CALASY

29. G. Montagna, O. Nicrosini and L. Trentadue, CERN-TH.5445/89 (1989)

30. T. Riemann and Z. Wąs, preprint MPI-PAE/PTh 34/89, München 1989

31. J.E. Campagne and R. Zitoun, "QED corrections to the forward-backward asymmetry at LEP energies", Preprint LPNHE - Paris (1988), to appear in Phys. Lett. B, and program COMPACT

32. D.R. Yennie, S.C. Frautschi and H. Suura, Annals of Phys. 13 (1961) 379

33. F.A. Berends, G. Burgers and W.L. van Neerven, Phys. Lett. 185 B (1987) 395; Nucl. Phys. B 297 (1988) 429; E: Nucl. Phys. B 304 (1988) 921

34. O. Nicrosini and L. Trentadue, Z. Phys. C 39 (1988) 479

35. J.E. Campagne and R. Zitoun, Z. Phys. C 43 (1989) 469

36. S. Jadach and B.F.L. Ward, Tennessee University Preprints UTHEP-88-0101, UTHEP-88-0201 (1988)

37. M. Consoli, W. Hollik and F. Jegerlehner, CERN-TH.5395/89 (1989), to appear in Phys. Lett. B